# Potential Energy and Spin−Spin Coupling Constants Surface of Glycolaldehyde

**Tomasz Ratajczyk, Magdalena Pecul,* and Joanna Sadlej**

*Department of Chemistry of Warsaw, Pasteura 1, 02-093 Warsaw, Poland*

**Trygve Helgaker**

*Department of Chemistry, University of Oslo, Box 1033, Blindern, N-0315 Oslo, Norway*

*Received: November 19, 2003; In Final Form: February 4, 2004*

The potential energy surface of the simplest carbohydrate, glycolaldehyde, was investigated at the second-order Møller−Plesset (MP2) level of theory, and the rotation barriers between them were calculated. Four local minima and six transition states were found. Next, the conformational dependence of the indirect nuclear spin−spin coupling constants was studied by means of density functional theory (DFT) using the B3LYP functional. For selected cases, the coupling constants calculated by means of DFT were compared with those obtained with coupled-cluster singles-and-doubles (CCSD) theory. The influence of rotation about the CC and CO bonds (with the remaining coordinates relaxed) on the spin−spin coupling constants was investigated, and the resulting curves were fit to a truncated Fourier series. The resulting expressions may help to determine the conformation of carbohydrates and their derivatives from the spin−spin coupling measurements. The relationships between coupling constants and dihedral angles were discussed and compared, whenever possible, with experimental trends.

## I. Introduction

Proton−proton vicinal spin−spin coupling constants have for a long time been used to resolve the 3D structure of biomolecules.[1−4] More recently, developments in nuclear magnetic resonance (NMR) techniques have allowed for the use of heteronuclear coupling constants for this purpose.[5,6] In particular, much work has focused on correlating the one-bond, geminal, and vicinal coupling constants of carbon, nitrogen, and even oxygen with molecular structure. (For reviews, see refs 5 and 6.) However, the determination of a given geometrical parameter from coupling constants is a nontrivial task because numerous factors influence the magnitude of the coupling constants, the molecular geometry being only one of these.[3,7]

In principle, theoretical calculations constitute a perfect tool for establishing the correlation of spectroscopic parameters with molecular structure because it is possible to model systems of interest in every possible conformation and every possible molecular environment. However, until recently, the ab initio calculation of coupling constants in systems of biochemical interest was practically impossible. The reasons were, on one hand, the inadequacy of the lowest-scaling ab initio method (the Hartree−Fock method) because of its frequent instability to triplet perturbations[8,9] and, on the other hand, the prohibitive cost of the methods that include electron correlation. With the recent development of methods for the calculation of spin−spin coupling constants using density functional theory (DFT),[10−14] with its low cost and less frequent instability problems,[8,9] this situation has changed dramatically. Nowadays, it has become possible to calculate spin−spin coupling constants—at least their dominant Fermi-contact contribution—in systems as large as pairs or triplets of nucleic bases[15,16] or even fullerene $C_{60}$.[17]

Not surprisingly, DFT has also been used for calculations of spin−spin coupling constants in saccharides and saccharide models such as xylopyranosides[18,19] or ethanediol.[6] However, the conformational dependence of the spin−spin coupling constants in models of carbohydrates has previously been evaluated only at the Hartree−Fock and simple configuration-interaction levels, raising doubts about the accuracy of the results.[20] To our knowledge, spin−spin coupling-constant surfaces have never been calculated for carbohydrate models in a way that accounts for molecular relaxation with changes in dihedral angles and at a level of theory that ensures at least semiquantitative accuracy, although such work has been carried out for peptide models.[21] The present work is designed to fill this gap. We investigate the potential energy surface of the simplest hydroxyaldehyde—glycolaldehyde—by calculating the surfaces of the spin−spin coupling constants generated by rotation about the C−C and C−O bonds.

Because glycolaldehyde represents both the smallest carbohydrate and one of the smallest stable systems with unhindered rotation around two single bonds, its potential energy surface has been investigated several times by means of theorical[22] as well as experimental[22−24] methods. The investigation of carbohydrate conformation is a pertinent subject, considering its biological importance and especially the presence of carbohydrate rings in nucleic acids. Moreover, because the glycolaldehyde molecule has been observed in interstellar space,[25] the investigation of its potential energy surface and, in particular, the identification of its local minima can be helpful in the interpretation of microwave and infrared spectra of interstellar matter.

In the present paper, we also address some issues concerning the methodology of spin−spin coupling calculations. In some cases, the performance of DFT for these constants is uncertain.[26] For selected conformers, the coupling constants have therefore also been calculated at the coupled-cluster singles-and-doubles (CCSD) level so as to benchmark the DFT results. In addition, a limited study of basis-set effects has been carried out. Of the

* Corresponding author. E-mail: mpecul@chem.uw.edu.pl.

10.1021/jp0375315 CCC: $27.50 © 2004 American Chemical Society
Published on Web 03/11/2004

four terms contributing to the spin−spin couplings constants, the Fermi-contact (FC) term, the paramagnetic spin−orbit (PSO) term, and the diamagnetic spin−orbit (DSO) term have been evaluated in all cases; in addition, the spin−dipole (SD) term has been evaluated at all equilibrium geometries. Although the FC term usually dominates the indirect spin−spin coupling constants, we consider this approach necessary because the changes in the PSO term may play a significant role in determining the shape of the spin−spin surfaces.[27,28]

The paper is organized as follows. First, the computational methods are described. Next, the calculated potential energy surface, in particular the stationary points and internal rotation barriers, is discussed. The coupling constants calculated for the global minimum at the DFT level are then compared with the CCSD results, and basis-set effects are considered. In the next subsection, the dependence of the glycolaldehyde coupling constants on the dihedral angles is discussed. Finally, a summary and the main conclusions are presented.

## II. Computational Method

**A. Geometry Optimization and Potential Energy Surface Calculations.** The geometry optimization and the calculation of the potential energy surface of glycolaldehyde were carried out at the frozen-core second-order Møller−Plesset (MP2) level as implemented in Gaussian 98[29] using the augmented correlation-consistent basis sets aug-cc-pVDZ and aug-cc-pVTZ of Dunning and co-workers.[30,31] For a uniform description of systems with and without internal hydrogen bonds, diffuse functions were added, being essential for a reliable rendering of electrostatic, induction, and dispersion interactions.

**B. Spin−Spin Coupling Constant Calculations.** The spin−spin coupling constants have been calculated at the DFT level using the hybrid Becke three-parameter Lee−Yang−Parr (B3LYP) functional,[32,33] as implemented in a local version of the DALTON program.[34] The DFT implementation is described in detail in refs 12 and 14. For selected structures, the coupling constants have also been calculated at the CCSD level using linear-response theory[35] as implemented in a program based on AcesII.[36] For a description of CCSD second derivatives in the unrestricted Hartree−Fock framework, see ref 37.

The calculations of the spin−spin coupling constants have been performed using the HII and HIII basis sets,[38] which contain the tight s functions necessary for these calculations. Additionally, we have used the HIII-su3 basis in which the original s basis has been uncontracted and augmented with three tight functions whose exponents form a geometric progression.[39] The use of several basis sets enables us to assess to some extent the effects of basis-set incompleteness and thus to estimate basis-set errors, as is necessary in any work aiming at semiqualitative accuracy. However, we note that in the CCSD calculations, in which dynamical correlation is described by means of virtual excitations, these basis sets are probably not sufficiently large to recover fully the effects of electron correlation.

## III. Results and Discussion

**A. Potential Energy Surface of Glycolaldehyde.** *1. Equilibrium Structures.* The structures corresponding to the stationary points on the potential energy surface of glycolaldehyde are shown in Figure 1. The corresponding energies (with zero-point vibrational corrections) relative to the lowest equilibrium structure CC are tabulated in Table 1.

On the potential energy surface of glycolaldehyde, we found four minima (denoted CC, TT, TG, and CT, where C, T, and G represent cis, trans, and gauche conformations, respectively, around C−C and C−O bonds) and six first-order saddle points (denoted TS1, TS2, TS3, TS4, TS5, and TS6). The structure corresponding to the conformation of the lowest-energy CC has been determined by microwave spectroscopy.[23] The calculated conformers of glycolaldehyde are consistent with previous experimental[23] and theoretical[22] results, although some of the structures found here have not been previously reported.

Whereas three of the local minima have $C_s$ symmetry, the TG minimum is asymmetric. There exists, naturally, an enantiomeric structure with an energy equal to that of TG, which will be denoted TG*. The global minimum CC is stabilized by an internal hydrogen bond. The TT and TG conformations are close in energy, having a similar configuration around the CC bond. The CT conformation, by contrast, has the structure with

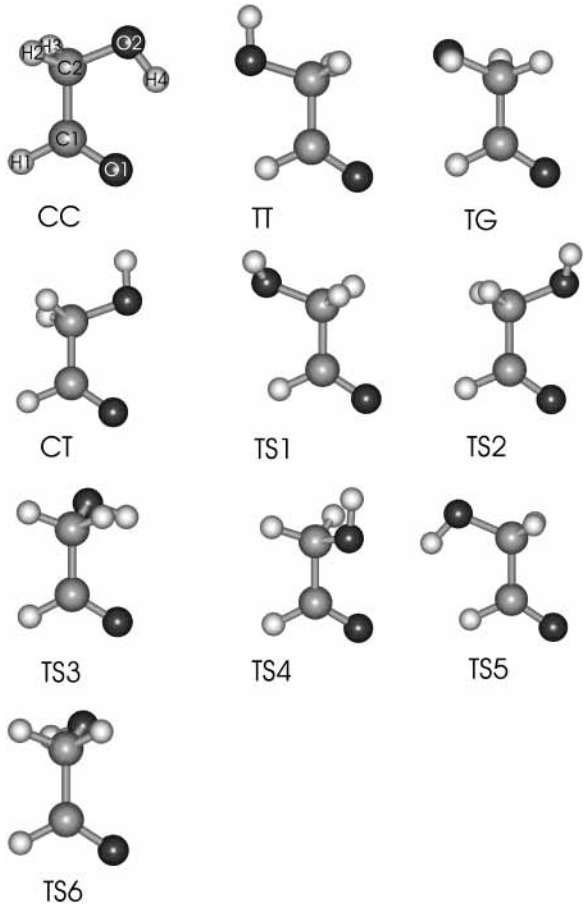


**Figure 1.** Structures corresponding to stationary points (local minima and transition states) of glycolaldehyde. Atomic numbering is shown for structure CC.

**TABLE 1: MP2 Energy (kJ/mol) of Glycolaldehyde Conformers with Respect to the Global Minimum CC**

| | aug-cc-pVDZ | | aug-cc-pVTZ | |
|---|---|---|---|---|
| | $\Delta E_e$[a] | $\Delta E_0$[b] | $\Delta E_e$[a] | $\Delta E_0$[b] |
| TT | 13.44 | 11.98 | 14.63 | 12.81 |
| TG | 14.22 | 12.92 | 15.39 | 13.94 |
| CT | 20.37 | 19.34 | 21.72 | 20.26 |
| TS1 | 16.74 | | 17.39 | |
| TS3 | 21.06 | | 22.89 | |
| TS2 | 23.33 | | 23.93 | |
| TS5 | 23.79 | | 24.30 | |
| TS6 | 32.43 | | 34.31 | |
| TS4 | 32.54 | | 34.59 | |

[a] Calculated without zero-point correction. [b] Calculated with zero-point correction.

the highest energy, with oxygen atoms in unfavorable cis positions and with no stabilizing hydrogen bonds. The geometric parameters of the stationary points and corresponding vibrational frequencies can be found in the Supporting Information.

Saddle points TS1, TS2, TS3, TS4, TS5, and TS6 correspond to the transition states between conformations TT and TG, CC and CT, CC and TG, TT and CT, TG and TG*, and CC and TG*, respectively. They are discussed in more detail below.

*2. Rotation Barriers.* There are two bonds in glycolaldehyde about which internal rotation is possible: C1−C2 and C2−O2. The rotational barriers have been calculated by carrying out partial geometry optimizations at the MP2/aug-cc-pVDZ level with the relevant dihedral angle ($\tau$(H1C1C2H2) or $\tau$(H2C2O2H4)) fixed at 15° intervals. With the $\tau$(H1C1C2H2) angle fixed, there are two possible orientations of the OH group: cis and trans. A similar situation arises with a fixed $\tau$(H2C2O2H4) angle. Therefore, two paths have been investigated for rotation about each bond.

For the rotation around C1−C2, the cc-1 path starts at the TT structure and $\tau$(C1C2O2H4) is close to 180° for each partially optimized structure, whereas the cc-2 path starts at the CC structure with $\tau$(C1C2O2H4) ≈ 0° for each structure. In fact, there are two different cc-2 paths: cc-2-r with the dihedral angle of $\tau$(C1C2O2H4) < 0° and cc-2-l with $\tau$(C1C2O2H4) > 0°. Paths cc-2-l and cc-2-r are mirror images of each other, crossing with $\tau$(H2C2O2H4) equal to 120° and 300° ($\tau$(H1C1C2O2) equal to 0° and 180°). In the CC basin, the constrained optimization resulted in only one local minimum, irrespective of the starting point.

The rotation around C2−O2 can also take place through two paths. In the case of the co-1 path, $\tau$(O1C1C2O2) is close to 180° as in the TT structure; for the co-2 path, it is close to 0° as in the CC structure. In principle, there are two different co-1 paths: one with $\tau$(O1C1C2O2) > 180° and one with $\tau$-(O1C1C2O2) < 180°. However, the deviations from 180° are so small that the structures are very close in energy, so we have not pursued this issue further.

The energies of the resulting cc-1, cc-2, co-1, and co-2 rotational paths have been plotted in Figure 2. In the following text, we shall discuss the corresponding barrier heights. The values referred to in the text have been obtained at the MP2/aug-cc-pVDZ level or at the MP2/aug-cc-pVTZ level (the numbers in parentheses).

The cc-1 rotation about the C1−C2 bond, with the hydroxylic hydrogen and aldehyde carbon atoms in the trans position, leads from TT to CT via the T4 transition state, with an energy barrier of 19.1 kJ/mol (20.0 kJ/mol). (See Figure 2a.) For the opposite transition from CT to TT through the enantiomeric T4* transition state, the barrier is 12.2 kJ/mol (12.9 kJ/mol).

The global minimum CC (Figure2b) is deeper, and the molecule needs 21.1 kJ/mol (22.9 kJ/mol) to undergo the cc-2 rotation about C1−C2 from CC to TG via TS3, the high barrier resulting from hydrogen bond breaking. Rotation about the C1−C2 bond in the same direction may also lead to enantiomeric state TG* via TS6. However, the corresponding barrier of 32.4 kJ/mol (34.3 kJ/mol) is very high, and the transition from CC to TG* by C1−C2 rotation in the opposite direction is favored. The transition from TG to TG* seems barrierless when only C1−C2 rotation is considered but in fact involves significant molecular rearrangements and for the cc-2 path does not go though a single transition state.

The co-1 potential energy curve associated with C2−O2 rotation, with the C1═O1 and C2−O2 bonds in the trans position, is shown in Figure 2c. The transition from TG to TG* via TS5 of $C_s$ symmetry has an energy barrier of 9.6 kJ/mol (8.9 kJ/mol). The transition from TG to TT via TS1 has a low energy barrier, 2.52 kJ/mol (2.00 kJ/mol), with a reverse barrier of 3.30 kJ/mol (2.76 kJ/mol). The highest barrier associated with the C2−O2 rotation, 23.33 kJ/mol (23.93 kJ/mol), accompanies the co-2 transition from CC to CT through TS2. (See Figure 2d.) The high barrier results from the breaking of the CC hydrogen bond. The reverse transition occurs over a barrier of only 2.96 kJ/mol (2.20 kJ/mol).

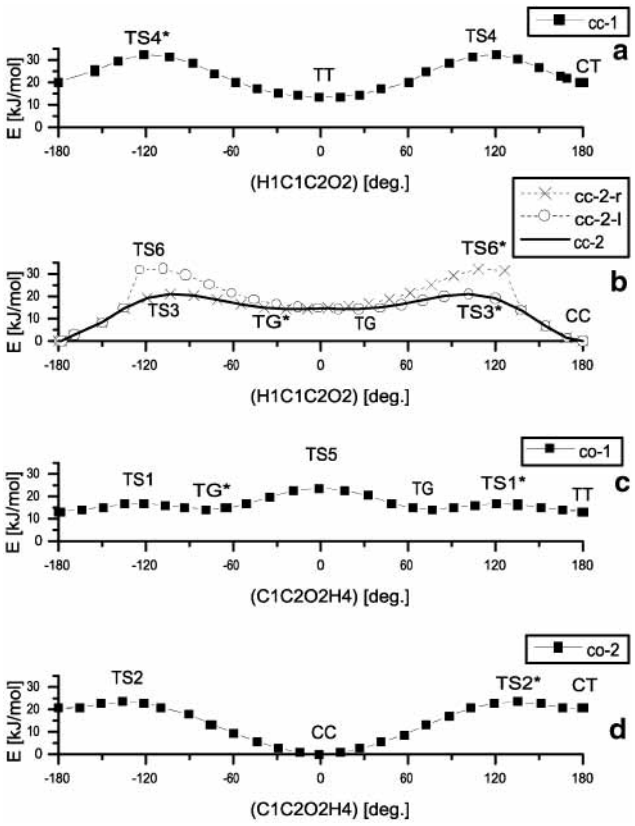


**Figure 2.** Potential energy curves resulting from rotation around (a) the C1−C2 bond with hydroxylic hydrogen and carbon atom in the trans position, cc-1, (b) the C1−C2 bond with hydroxylic hydrogen and carbon atom in the cis position, cc-2, (c) the C2−O2 bond with oxygen atoms in the trans position, co-1, and (d) the C2−O2 bond with oxygen atoms in the cis position, co-2.

**B. Spin−Spin Coupling Constants: Methodological Issues.** *1. Comparison of DFT against CCSD Results.* Selected spin−spin coupling constants of glycolaldehyde, calculated at the DFT and CCSD levels of theory, are presented in Table 2. The results have been obtained with the HII basis, the CCSD calculations in a larger basis being too expensive. However, we note that the HII basis is far from ideal for the CCSD calculations, lacking the high-angular-momentum functions needed to recover electron correlation in this method. With no need for correlating orbitals, DFT has much lower basis-set requirements than CCSD, which should be kept in mind when comparing the results.

As seen from Table 2, the DFT and CCSD coupling constants of glycolaldehyde are close to each other. More importantly, the differences in the coupling constants between the CC and TT structures are almost identical at the DFT and CCSD levels of theory, indicating yet again that DFT is suitable for the calculation of the conformational dependence of coupling constants. The largest differences between DFT and CCSD occur for oxygen: the $^1J_{CO}$ couplings appear to be overestimated at

**TABLE 2: Individual Contributions to the Spin−Spin Coupling Constants (Hz) in Glycolaldehyde Calculated at DFT/B3LYP and CCSD Computational Levels Using the HII Basis Set[a]**

| | FC | | PSO | | DSO | | SD | |
|---|---|---|---|---|---|---|---|---|
| | DFT | CCSD | DFT | CCSD | DFT | CCSD | DFT | CCSD |
| | | | | CC Structure | | | | |
| $^1J_{CC}$ | 37.01 | 40.84 | −2.55 | −1.85 | 0.25 | 0.25 | 0.60 | 0.69 |
| $^1J_{CO^h}$ | 27.43 | 19.26 | −0.08 | −0.61 | −0.10 | −0.10 | −1.46 | −1.37 |
| $^1J_{CO^a}$ | 22.35 | 15.14 | 20.64 | 18.46 | −0.05 | −0.05 | −2.55 | −1.91 |
| $^1J_{OH}$ | −56.14 | −66.05 | −9.34 | −8.74 | −0.39 | −0.40 | −0.25 | −0.21 |
| $^1J_{CH^m}$ | 140.63 | 132.05 | 0.04 | −0.01 | 0.94 | 0.94 | 0.12 | 0.01 |
| $^1J_{CH^a}$ | 174.03 | 164.28 | −1.25 | −1.10 | 0.94 | 0.95 | 0.34 | 0.15 |
| $^2J_{CH^h}$ | −3.23 | −4.47 | 0.66 | 0.71 | −0.42 | −0.42 | 0.05 | 0.06 |
| $^2J_{CH^m}$ | −3.15 | −5.03 | −0.16 | −0.12 | −0.01 | −0.01 | 0.16 | 0.13 |
| $^2J_{CH^a}$ | 29.50 | 25.66 | −0.15 | −0.07 | −0.20 | −0.20 | 0.02 | 0.02 |
| $^2J_{HH}$ | −22.29 | −18.89 | 1.99 | 1.94 | −2.05 | −2.04 | 0.36 | 0.37 |
| $^3J_{CH^h}$ | 7.90 | 6.89 | −0.81 | −0.73 | 0.25 | 0.25 | −0.09 | −0.09 |
| $^3J_{H^mH^h}$ | 3.93 | 3.12 | 2.99 | 2.91 | −3.23 | −3.22 | −0.04 | −0.04 |
| $^3J_{H^mH^a}$ | −0.24 | −0.15 | 0.44 | 0.43 | −0.51 | −0.51 | 0.11 | 0.10 |
| $^4J_{HH}$ | 1.07 | 0.60 | 1.78 | 1.76 | −2.06 | −2.06 | −0.02 | −0.02 |
| | | | | TT Structure | | | | |
| $^1J_{CC}$ | 48.72 | 51.92 | −2.03 | −1.46 | 0.24 | 0.24 | 0.75 | 0.81 |
| $^1J_{CO^h}$ | 24.75 | 16.70 | −1.46 | −1.67 | −0.09 | −0.09 | −1.80 | −1.63 |
| $^1J_{CO^a}$ | 21.28 | 14.02 | 21.46 | 18.95 | −0.04 | −0.04 | −2.76 | −2.02 |
| $^1J_{OH}$ | −55.63 | −66.40 | −11.16 | −10.22 | −0.32 | −0.33 | −0.45 | −0.38 |
| $^1J_{CH^m}$ | 140.16 | 132.19 | −0.04 | −0.08 | 0.92 | 0.93 | 0.16 | 0.05 |
| $^1J_{CH^a}$ | 178.24 | 167.92 | −1.33 | −1.15 | 0.99 | 1.00 | 0.41 | 0.20 |
| $^2J_{CH^h}$ | −1.83 | −2.94 | 0.69 | 0.74 | −0.57 | −0.57 | 0.04 | 0.04 |
| $^2J_{CH^m}$ | −5.04 | −6.35 | −0.06 | −0.04 | −0.04 | −0.04 | 0.12 | 0.10 |
| $^2J_{CH^a}$ | 21.97 | 19.34 | −0.05 | 0.02 | −0.20 | −0.20 | 0.03 | 0.03 |
| $^2J_{HH}$ | −16.79 | −14.94 | 2.06 | 2.01 | −2.12 | −2.10 | 0.33 | 0.34 |
| $^3J_{CH^h}$ | 14.61 | 12.41 | 0.57 | 0.57 | −0.68 | −0.67 | 0.04 | 0.03 |
| $^3J_{H^mH^h}$ | 1.03 | 0.81 | 0.84 | 0.81 | −1.07 | −1.07 | 0.06 | 0.06 |
| $^3J_{H^mH^a}$ | 1.12 | 0.96 | 1.97 | 1.93 | −2.15 | −2.15 | −0.03 | −0.02 |
| $^4J_{HH}$ | −0.41 | −0.37 | 2.67 | 2.62 | −2.81 | −2.80 | −0.02 | −0.02 |

[a] Superscripts h, m, and a denote the atoms of hydroxyl, methylene, and aldehyde groups, respectively.

the DFT level, but $^1J_{OH}$ is underestimated (in terms of absolute value) by DFT. These observations are consistent with previous findings—DFT is usually less reliable for coupling constants of electron-rich atoms such as oxygen and, in particular, fluorine,[26,40,41] although there are exceptions such as the fluorine−fluorine couplings in substituted aromatic compounds (usually dominated by the PSO term).[42] For $^1J_{CO}$ and $^1J_{OH}$ in glycolaldehyde, we may therefore assume that the CCSD constants are closer to the true values than the DFT constants are. We are not aware of any experimental measurements of oxygen couplings in glycolaldehyde. However, we note that the experimental value of $^1J_{OH}$ in methanol (85 ± 10 Hz, sign unknown)[43] is closer to the CCSD value than to the DFT value.[40]

As observed for the other systems,[40] the coupling constants to protons and carbons are well reproduced by DFT. In particular, we note that the positive sign of the $^2J_{CH^a}$ coupling of the aldehyde proton, typical of geminal couplings mediated by a carbonyl carbon,[6] is reproduced by DFT as well as by CCSD. Both methods are in a reasonable agreement with experiment; we note that $^2J_{CH^a}$ in acetaldehyde has been measured at 26.25 Hz in DMSO and at 29.54 Hz in the gas phase.[44] The magnitude of the $^2J_{CH}$ geminal couplings calculated by CCSD and DFT differ by nearly 50% in some cases; however, in view of the different basis-set requirements of the two methods, this is not necessarily an indication of the failure of DFT.

Whenever discrepancies between DFT and CCSD total couplings occur, they are caused by the FC term. For some couplings such as $^1J_{CC}$, large differences are also observed for the PSO and SD terms, but this hardly matters because both terms contribute little to the overall coupling. As usual,[40,41] the DSO term is practically the same at the DFT and CCSD levels of theory.

Except for the $^1J_{CO}$ couplings and some proton−proton couplings, the coupling constants in Table 2 are dominated by the FC term, which also contributes the most to the differences between the couplings in CC and TT structures. However, it has previously been shown[27,28] that torsional motion about C−C or C−O bonds predominantly influences the PSO term of the coupling constant between the nuclei of the rotational axis. We therefore decided to calculate the spin−orbit terms in addition to the FC term. Because the SD term is very small in all cases and also the most expensive one, we decided to omit it from the analysis of the conformational dependence of the coupling constants, although we note that the relative variation of the (small) SD term is quite substantial for some couplings in glycolaldehyde.

*2. Basis-Set Effects.* The individual contributions to the DFT spin−spin coupling constants in CC and TT conformations of glycolaldehyde calculated with different basis sets are tabulated in Table 3. We investigate here the performance of the HII basis, the HIII basis, differing from the HII basis in the number of polarization functions, and the HIII-su3 basis, with uncontracted s orbitals and with three tight s functions added.

The coupling constants calculated in the three basis sets are quite similar. In general, the coupling constants between two heavy atoms are most affected by the addition of polarization functions (compare the HII and HIII results), which improve the flexibility of the one-electron density description, whereas the proton coupling constants are more sensitive to the quality of the core description (compare the HIII and HIII-su3 results). The addition of tight s functions predominantly influences the FC term, as does the change from HII and HIII. The effects on the PSO term are smaller, and those on the DSO and SD terms are negligible. Basis-set requirements for the spin−spin coupling constants have been studied in more detail in refs 39 and 45.

It is gratifying to note that, for a given coupling constant, the difference between CC and TT structures, that is, the effect of a conformational change, does not depend strongly on the basis set. In particular, the HIII and HIII-su3 results are very close to each other in this respect. For $^1J_{CH^m}$, the difference between the CC and TT values in the HII basis set differs from the HIII and HIII-su3 results. The angular dependence of the coupling constants has therefore been studied in the HIII basis.

**C. Spin−Spin Coupling Constants: Conformational Dependence.** *1. Effects of Internal Rotations on the Spin−Spin Coupling Constants in Glycolaldehyde.* We here discuss the dependence of the coupling constants of glycolaldehyde on the dihedral angles by analyzing the data obtained for several structures on pathways cc-1, cc-2, co-1, and co-2, optimized with either the $\tau$(H1C1C2H2) or $\tau$(H2C2O2H4) dihedral angle frozen. We focus on the coupling constants that exhibit a substantial variation with the geometry and that are accessible by experimental NMR techniques. For example, even though all couplings have been calculated, we do not discuss the $^1J_{CO}$ coupling constants, which are practically unattainable by NMR. The calculated coupling constants were fit to a truncated Fourier series, containing at most five terms, in a least-squares manner. The truncated Fourier series seem appropriate for the fitting dependence of most of the calculated coupling constants on the dihedral angles. For smooth and relatively small changes in the one-bond coupling constants (see below), the fitting error does

**TABLE 3: Individual Contributions to the Spin−Spin Coupling Constants (Hz) in Glycolaldehyde Calculated at the DFT/B3LYP Computational Level Using HII, HIII, and HIII-su3 Basis Sets[a]**

| | FC | | | PSO | | | DSO | | | SD | | |
|---|---|---|---|---|---|---|---|---|---|---|---|---|
| | HII | HIII | HIII-su3 | HII | HIII | HIII-su3 | HII | HIII | HIII-su3 | HII | HIII | HIII-su3 |
| | | | | | | CC Structure | | | | | | |
| $^1J_{CC}$ | 37.01 | 35.21 | 36.46 | −2.73 | −2.73 | −2.55 | 0.25 | 0.25 | 0.25 | 0.61 | 0.61 | 0.60 |
| $^1J_{CO^h}$ | 27.43 | 25.53 | 25.81 | −0.02 | −0.02 | −0.08 | −0.09 | −0.09 | −0.10 | −1.52 | −1.52 | −1.46 |
| $^1J_{CO^a}$ | 22.35 | 19.87 | 19.87 | 21.14 | 21.14 | 20.64 | −0.05 | −0.05 | −0.05 | −2.53 | −2.53 | −2.55 |
| $^1J_{OH}$ | −56.14 | −60.11 | −65.20 | −9.49 | −9.50 | −9.34 | −0.35 | −0.35 | −0.39 | −0.26 | −0.27 | −0.25 |
| $^1J_{CH^m}$ | 140.63 | 140.52 | 151.71 | 0.15 | 0.15 | 0.04 | 0.91 | 0.91 | 0.94 | −0.13 | −0.12 | 0.12 |
| $^1J_{CH^a}$ | 174.03 | 174.62 | 189.01 | −1.23 | −1.23 | −1.25 | 0.91 | 0.91 | 0.94 | 0.16 | 0.17 | 0.34 |
| $^2J_{CH^h}$ | −3.23 | −2.85 | −3.17 | 0.68 | 0.68 | 0.66 | −0.43 | −0.43 | −0.42 | 0.07 | 0.07 | 0.05 |
| $^2J_{CH^m}$ | −3.15 | −2.54 | −3.13 | −0.16 | −0.16 | −0.16 | −0.02 | −0.02 | −0.01 | 0.19 | 0.19 | 0.16 |
| $^2J_{CH^a}$ | 29.50 | 30.54 | 32.88 | −0.17 | −0.17 | −0.15 | −0.20 | −0.20 | −0.20 | 0.03 | 0.03 | 0.02 |
| $^2J_{HH}$ | −22.29 | −22.14 | −25.83 | 2.15 | 2.15 | 1.99 | −2.13 | −2.13 | −2.05 | 0.48 | 0.48 | 0.36 |
| $^3J_{CH^h}$ | 7.90 | 7.82 | 8.29 | −0.84 | −0.84 | −0.81 | 0.24 | 0.24 | 0.25 | −0.09 | −0.09 | −0.09 |
| $^3J_{H^mH^h}$ | 3.93 | 3.97 | 4.64 | 3.23 | 3.23 | 2.99 | −3.26 | −3.26 | −3.23 | −0.02 | −0.02 | −0.04 |
| $^3J_{H^mH^a}$ | −0.24 | −0.54 | −0.52 | 0.49 | 0.49 | 0.44 | −0.53 | −0.53 | −0.51 | 0.10 | 0.10 | 0.11 |
| $^4J_{HH}$ | 1.07 | 1.28 | 1.41 | 1.92 | 1.92 | 1.78 | −2.08 | −2.08 | −2.06 | −0.03 | −0.03 | −0.02 |
| | | | | | | TT Structure | | | | | | |
| $^1J_{CC}$ | 48.72 | 45.77 | 47.25 | −2.03 | −2.17 | −2.17 | 0.24 | 0.25 | 0.25 | 0.75 | 0.78 | 0.78 |
| $^1J_{CO^h}$ | 24.75 | 22.93 | 23.19 | −1.46 | −1.53 | −1.53 | −0.09 | −0.09 | −0.09 | −1.80 | −1.90 | −1.90 |
| $^1J_{CO^a}$ | 21.28 | 18.98 | 18.94 | 21.46 | 22.05 | 22.05 | −0.04 | −0.04 | −0.04 | −2.76 | −2.76 | −2.76 |
| $^1J_{OH}$ | −55.63 | −59.66 | −64.71 | −11.16 | −11.44 | −11.44 | −0.32 | −0.27 | −0.27 | −0.45 | −0.53 | −0.53 |
| $^1J_{CH^m}$ | 140.16 | 141.20 | 152.48 | −0.04 | 0.05 | 0.05 | 0.92 | 0.89 | 0.89 | 0.16 | −0.09 | −0.08 |
| $^1J_{CH^a}$ | 178.24 | 178.31 | 193.02 | −1.33 | −1.33 | −1.33 | 0.99 | 0.96 | 0.96 | 0.41 | 0.24 | 0.24 |
| $^2J_{CH^h}$ | −1.83 | −1.38 | −1.62 | 0.69 | 0.76 | 0.76 | −0.57 | −0.58 | −0.58 | 0.04 | 0.05 | 0.05 |
| $^2J_{CH^m}$ | −5.04 | −4.69 | −5.36 | −0.06 | −0.06 | −0.06 | −0.04 | −0.04 | −0.04 | 0.12 | 0.15 | 0.15 |
| $^2J_{CH^a}$ | 21.97 | 22.60 | 24.33 | −0.05 | −0.05 | −0.05 | −0.20 | −0.21 | −0.21 | 0.03 | 0.04 | 0.04 |
| $^2J_{HH}$ | −16.79 | −16.65 | −19.54 | 2.06 | 2.23 | 2.23 | −2.12 | −2.19 | −2.19 | 0.33 | 0.45 | 0.45 |
| $^3J_{CH^h}$ | 14.61 | 14.35 | 15.35 | 0.57 | 0.60 | 0.60 | −0.68 | −0.68 | −0.68 | 0.04 | 0.04 | 0.04 |
| $^3J_{H^mH^h}$ | 1.03 | 0.98 | 1.07 | 0.84 | 0.98 | 0.98 | −1.07 | −1.10 | −1.10 | 0.06 | 0.05 | 0.05 |
| $^3J_{H^mH^a}$ | 1.12 | 1.11 | 1.22 | 1.97 | 2.11 | 2.11 | −2.15 | −2.18 | −2.18 | −0.03 | −0.02 | −0.02 |
| $^4J_{HH}$ | −0.41 | −0.48 | −0.52 | 2.67 | 2.86 | 2.86 | −2.81 | −2.83 | −2.83 | −0.02 | −0.02 | −0.02 |

[a] Superscripts h, m, and a denote the atoms of hydroxyl, methylene, and aldehyde groups, respectively.

not typically exceed 2−3% of the value of the coupling. The maximum fitting error is larger for the geminal couplings (even up to 10−15% close to the extrema). For the vicinal coupling constants, it typically does not exceed 0.5 Hz (because the changes in $^3J_{HH}$ and $^3J_{CH}$ span a wide range, the absolute value in more informative in this case). However, we did not attempt to fit the cc-2 curves because these are mostly discontinuous, being superpositions of the cc-2-r and cc-2-l paths.

*a. $^1J_{CH}$ One-Bond Coupling Constants.* In Figure 3, we have plotted the dependence of the $^1J_{CH^m}$ coupling of the methylene proton on the conformation around C1−C2 or C2−O2—that is, on the dihedral angle $\tau$(H1C1C2H2) or $\tau$(H1C1C2H3) for cc-1 and cc-2 and on the dihedral angle $\tau$(H2C2O2H4) or $\tau$(H3C2O2H4) for co-1 and co-2, respectively. There are two such couplings, which are nonequivalent for asymmetric structures. Both are plotted as functions of the dihedral angles in Figure 3.

As pointed out several times,[46−48] these coupling constants are particularly sensitive to electric-field effects and, consequently, to the orientation of lone pairs at nearby electronegative atoms. (See Figure 3.) Concerning the rotation about the C1−C2 bond, the largest values are assumed by $^1J_{CH^m}$ when $\tau$(H1C1C2H2(H3) ≈ 180°—that is, when the coupled proton is in the cis orientation with respect to the carbonyl oxygen. Conversely, the minimum occurs when the dihedral angle between the C2−H2(H3) bond and the carbonyl group is close to 90°. A second and usually lower maximum occurs at a trans orientation of the coupled proton relative to the carbonyl group; this is consistent with theoretical findings for acetaldehyde and with experimental results,[6] although the dependence is different

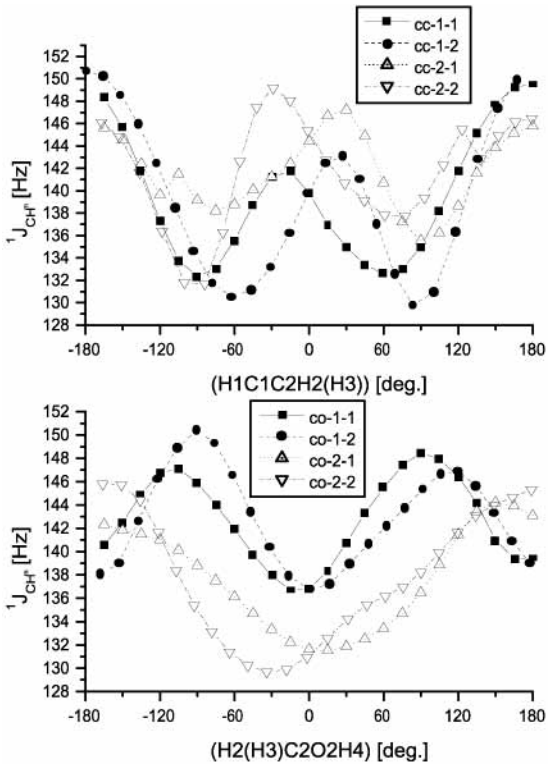


**Figure 3.** $^1J_{CH^m}$ coupling constant of the methylene proton (in Hz) as a function of the dihedral angle $\tau$(H1C1C2H2) (or $\tau$(H1C1C2H3)) or $\tau$(H2C2O2H4) (or $\tau$(H3C2O2H4)) (in deg).

for the cc-1 and cc-2 curves. The cc-1-1 and cc-1-2 curves can be represented by the following truncated Fourier series:

$$\text{cc-1-1: } {}^1J_{CH^m}(\text{Hz}) = 139.45 - 5.01\cos(\tau) + 5.51\cos(2\tau) + 0.31\sin(\tau) - 2.30\sin(2\tau) \quad (1)$$

$$\text{cc-1-2: } {}^1J_{CH^m}(\text{Hz}) = 139.20 - 5.53\cos(\tau) + 6.70\cos(2\tau) - 0.04\sin(\tau) + 3.01\sin(2\tau) \quad (2)$$

The curves corresponding to the cc-2 path are discontinuous where cc-2-l and cc-2-r cross. (See Figure 2.)

Rotation about the C2−O2 bond also has a large influence on the ${}^1J_{CH^m}$ coupling. This phenomenon, interpreted as the influence of lone pairs of the electronegative substituent in the α position on the ${}^1J_{CH}$ coupling, is the well-known Perlin effect,[6,44] observed several times in carbohydrates. In the case of the co-1 curve, the dependence of ${}^1J_{CH^m}$ on the dihedral angle is similar to that in methanol:[6,28] the coupling goes through a minimum when $\tau$(H2(H3)C2O2H4) is 0 or 180° and assumes maximum values for +90° and close to −90°. However, there is asymmetry in the values for 0 and 180° and for 90 and −90°, probably because of the influence of the carbonyl group. The dependence of ${}^1J_{CH}$ on $\tau$(H2(H3)C2O2H4) can be fitted by the following equations:

$$\text{co-1-1: } {}^1J_{CH^m}(\text{Hz}) = 142.79 - 1.64\cos(\tau) - 4.54\cos(2\tau) + 1.01\sin(\tau) + 1.17\sin(2\tau) \quad (3)$$

$$\text{co-1-2: } {}^1J_{CH^m}(\text{Hz}) = 142.83 - 1.39\cos(\tau) - 5.02\cos(2\tau) - 1.26\sin(\tau) - 1.40\sin(2\tau) \quad (4)$$

$$\text{co-2-1: } {}^1J_{CH^m}(\text{Hz}) = 137.77 - 6.00\cos(\tau) - 0.17\cos(2\tau) - 0.65\sin(\tau) - 1.01\sin(2\tau) \quad (5)$$

$$\text{co-2-2: } {}^1J_{CH^m}(\text{Hz}) = 137.78 - 7.46\cos(\tau) + 0.82\cos(2\tau) + 1.56\sin(\tau) + 1.56\sin(2\tau) \quad (6)$$

Interesting effects of internal rotation can be observed for the coupling to the aldehyde proton ${}^1J_{CH^a}$ in Figure 4. The dependence of this constant on $\tau$(H1C1C2O2) is weak, especially for the cc-2 curve, although the maximum for the CC conformation at 180° is clearly visible. In the cc-1 curve, the dependence of ${}^1J_{CH^a}$ on $\tau$(H1C1C2O2) is stronger, with a maximum for the TT structure ($\tau$ = 0°), where the aldehyde C−H and C−O bonds are in the cis conformation, and a minimum for the trans CT structure. The interaction of the aldehyde hydrogen with the hydroxylic oxygen lone pairs then increases ${}^1J_{CH^a}$, although the dependence differs from that observed above when the influence of the carbonyl group on the methylene couplings was considered. The changes in ${}^1J_{CH^a}$ with rotation about the C−C bond are described by the equation

$$\text{cc-1: } {}^1J_{CH^a}(\text{Hz}) = 174.01 + 3.44\cos(\tau) - 0.64\cos(2\tau) + 1.03\cos(3\tau) \quad (7)$$

Rather unexpectedly, significant changes in ${}^1J_{CH^a}$ are induced by rotation about the C2−O2 bond. In the co-2 curve, there are maxima for the CC (0°) and CT (180°) structures, where C1−H1 and C2−O2 bonds are coplanar. For the co-1 curve, the dependence on the rotation is even stronger because of the proximity of the aldehyde proton and the hydroxyl oxygen. The ${}^1J_{CH^a}$ minimum is observed for the TS5 transition state (0°), probably because of steric repulsion between the hydroxyl and aldehyde hydrogen atoms, which are close to each other in this

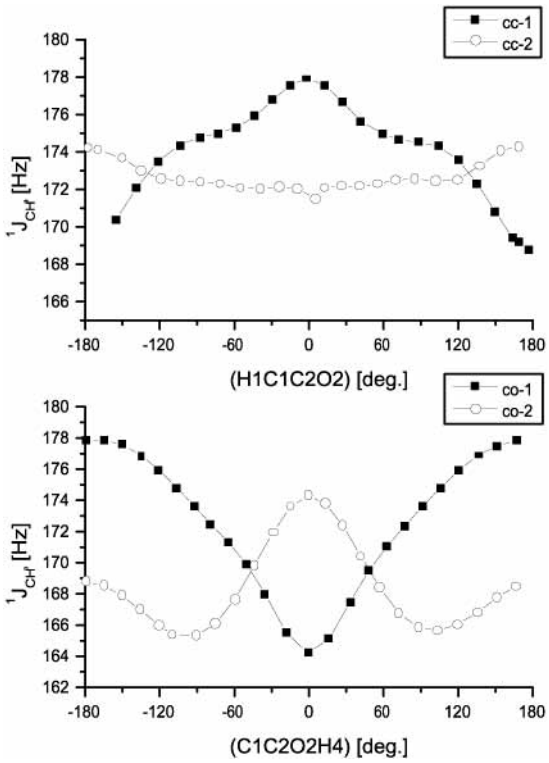


**Figure 4.** ${}^1J_{CH^a}$ coupling constant of the aldehyde proton (in Hz) as a function of the dihedral angle $\tau$(H1C1C2O2) or $\tau$(C1C2O2H4) (in deg).

structure. The ${}^1J_{CH^a}$ maximum occurs for TT (180°), and at least two effects appear to be at play, namely, the electrostatic influence of the oxygen lone pairs and the steric repulsion of the hydroxyl hydrogen atom. For the rotation about the C2−O2 bond, the equations describing the dependence of ${}^1J_{CH^a}$ on $\tau$ (C1C2O2H4) are given by

$$\text{co-1: } {}^1J_{CH^a}(\text{Hz}) = 172.64 - 6.13\cos(\tau) - 1.16\cos(2\tau) - 0.59\cos(3\tau) \quad (8)$$

$$\text{co-2: } {}^1J_{CH^a}(\text{Hz}) = 168.43 + 2.42\cos(\tau) + 2.97\cos(2\tau) + 0.30\cos(3\tau) \quad (9)$$

*b.* ${}^1J_{CC}$ *One-Bond Coupling Constant.* The variation of ${}^1J_{CC}$ with $\tau$(H1C1C2O2) and $\tau$(C1C2O2H4) is depicted in Figure 5. Rotation about the C1−C2 bond influences ${}^1J_{CC}$ significantly, especially for the cc-2 path. For both the cc-1 path and the cc-2 path, there is a minimum in ${}^1J_{CC}$ when the C1═O1 and C2−O2 bonds are in cis positions (for $\tau$(H1C1C2O2) = 180°, CT and CC structures, respectively). The minimum of the ${}^1J_{CC}$ curve is much deeper for cc-2 than for cc-1, which may reflect the influence of the internal hydrogen bond in the CC structure on the cc-2 path. The value of ${}^1J_{CC}$ correlates inversely with the C1−C2 bond length for the cc-1 path. This is not the case with the cc-2 path, where the methylene C1−H1(H2) bond lengths undergo substantial changes, strongly influencing ${}^1J_{CC}$. The changes in ${}^1J_{CC}$ along the cc-1 path can be described by the relation

$$\text{cc-1: } {}^1J_{CC}(\text{Hz}) = 43.25 + 1.66\cos(\tau) - 0.90\cos(2\tau) - 0.18\cos(3\tau) \quad (10)$$

Next, we turn our attention to the co-1 and co-2 curves. During the rotation about the C2−O2 bond, ${}^1J_{CC}$ changes by several hertz, assuming its minimum value with C1−C2 and O2−H4 in the cis conformation (0°, CC and TS5 structures,

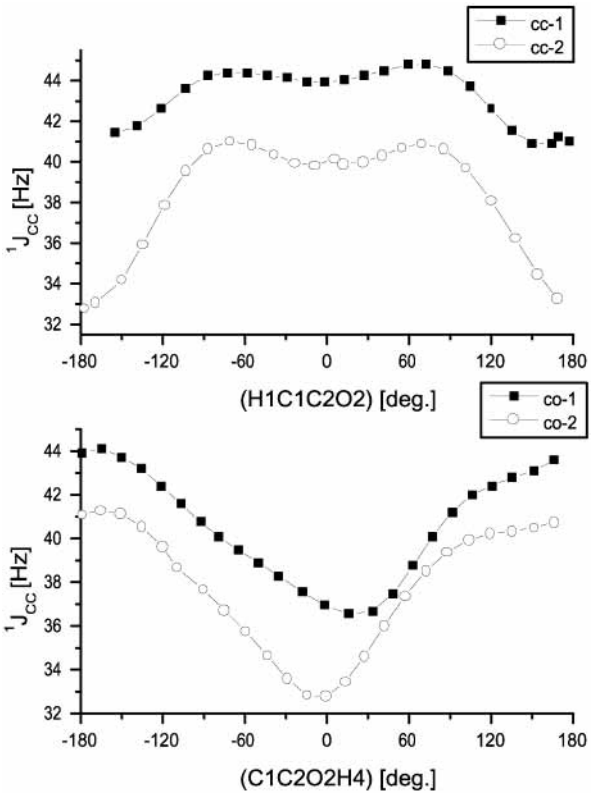


**Figure 5.** $^1J_{CC}$ coupling constant (in Hz) as a function of the dihedral angle $\tau$(H1C1C2O2) or $\tau$(C1C2O2H4) (in deg).

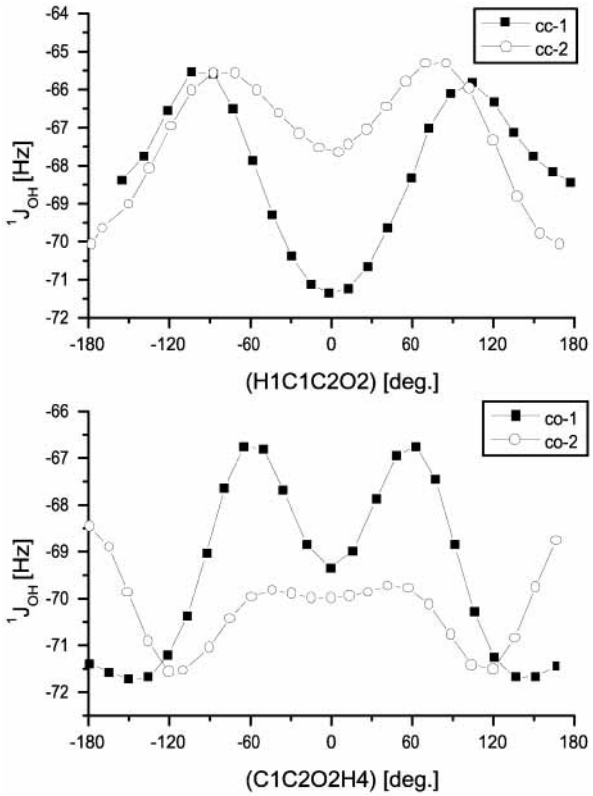


**Figure 6.** $^1J_{OH}$ coupling constant (in Hz) as a function of the dihedral angle $\tau$(H1C1C2O2) or $\tau$(C1C2O2H4) (in deg).

respectively) and its maximum when these bonds are in the trans position (180°, TT and CT structures, respectively). The co-1 and co-2 curves are nearly parallel to each other. The effect of internal rotation about the C−O bond on $^1J_{CC}$ can be treated by analogy to the Perlin effect on $^1J_{CH}$.[6,44] The dependence of $^1J_{CC}$ on the $\tau$(H1C1C2O2) and $\tau$(C1C2O2H4) dihedral angles, respectively, can be described by the following equations:

$$\text{cc-1: } {}^1J_{CC}(\text{Hz}) = 37.85 - 3.78\cos(\tau) - 0.79\cos(2\tau) - 0.34\cos(3\tau) \quad (11)$$

$$\text{co-2: } {}^1J_{CC}(\text{Hz}) = 37.86 - 3.81\cos(\tau) - 0.79\cos(2\tau) - 0.32\cos(3\tau) + 0.72\sin(\tau) \quad (12)$$

The large changes in $^1J_{CC}$ with $\tau$(H1C1C2O2) and $\tau$-(C1C2O2H4) illustrate the potential of $^1J_{CC}$ coupling constants as probes of molecular conformation. At the same time, any conclusions should be drawn with caution because these couplings are also strongly influenced by changes in adjacent bond lengths. Finally, the effects of internal rotation on $^1J_{CC}$ and on $^1J_{CO}$ in glycolaldehyde are dominated by the FC term, unlike the situation in ethane and in methanol,[27,28] respectively, where changes in the PSO term are the most important ones.

*c. $^1J_{OH}$ One-Bond Coupling Constant.* The $^1J_{OH}$ coupling constants are difficult to measure because of the quadrupolar character of the $^{17}$O nucleus, its low natural abundance, and the exchange of the hydroxylic proton with hydrogen bond-forming solvent molecules. However, if the measurements are possible, then the $^1J_{OH}$ couplings may provide invaluable information, especially on hydrogen bonds.

The dependence of $^1J_{OH}$ on $\tau$(H1C1C2O2) and $\tau$(C1C2O2H4) is illustrated in Figure 6. The changes in $^1J_{OH}$ span a range of approximately 6 Hz, with the smallest absolute values observed when the hydroxyl proton lies outside of the plane formed by the C−C bond and the aldehyde group. Conversely, when the O2−H4 bond lies in the plane with the C1−C2 bond, as in the TT, CC, and TS5 structures, the $^1J_{OH}$ coupling has the largest absolute values. In most cases, therefore, the extrema of $^1J_{OH}$ coincide with the stationary points on the potential energy curves. Somewhat surprisingly, the formation of the internal hydrogen bond in the CC structure does not strongly influence the $^1J_{OH}$ coupling. The dependence of $^1J_{OH}$ on $\tau$(H1C1C2O2) and $\tau$(C1C2O2H4), respectively, is described by the following equations:

$$\text{cc-1: } {}^1J_{OH}(\text{Hz}) = -68.07 + 1.45\cos(\tau) - 2.06\cos(2\tau) + 0.02\cos(3\tau) \quad (13)$$

$$\text{co-1: } {}^1J_{OH}(\text{Hz}) = -69.46 + 2.14\cos(\tau) - 0.86\cos(2\tau) - 1.17\cos(3\tau) \quad (14)$$

$$\text{co-2: } {}^1J_{OH}(\text{Hz}) = -70.22 + 0.02\cos(\tau) + 0.86\cos(2\tau) - 0.80\cos(3\tau) \quad (15)$$

*d. $^2J_{CH}$ Geminal Coupling Constants.* There are three different types of $^2J_{CH}$ coupling constants in glycolaldehyde, which will be discussed in this paragraph.

The strong dependence of the $^2J_{CH}$ coupling of the carbonyl carbon (here $^2J_{CH^m}$) on the conformation of the carbonyl group is well documented.[6] The changes in $^2J_{CH^m}$ with rotation about the C1−C2 bond are depicted in Figure 7. For the cc-1 path, the $^2J_{CH^m}$ value is the least negative and close to zero when the carbonyl group is in the trans position relative to the C2−H2-(H3) bond of the coupled proton ($\tau = 0°$) and the most negative when $\tau \approx 90°$. The dependence on the appropriate dihedral angle ($\tau$(H1C1C2H2) or $\tau$(H1C1C2H3)) is given by the following

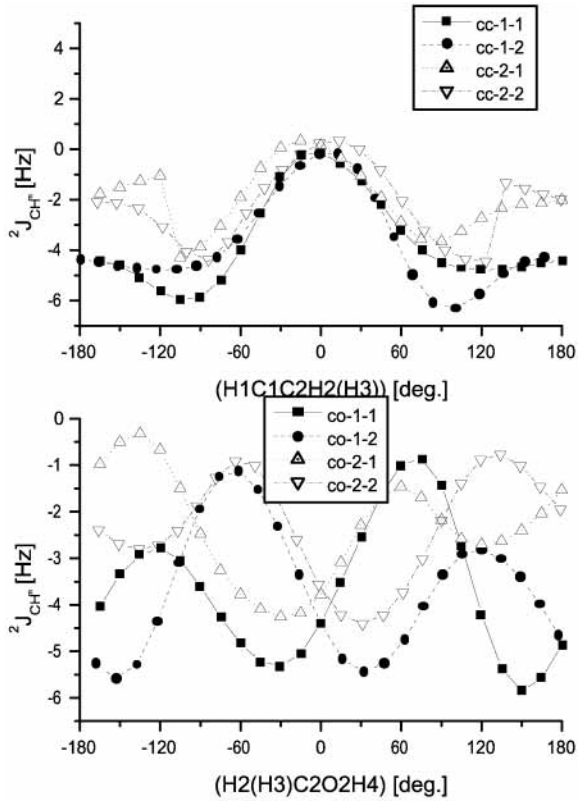


**Figure 7.** $^2J_{CH^m}$ coupling constant (in Hz) as a function of the dihedral angle $\tau$(H1C1C2H2) (or $\tau$(H1C1C2H3)) or $\tau$(H2C2O2H4) (or $\tau$-(H3C2O2H4)) (in deg).

equations:

$$\text{cc-1-1: } {}^2J_{CH^m}(\text{Hz}) = -3.69 + 1.97\cos(\tau) + 1.47\cos(2\tau) + 0.18\cos(3\tau) + 0.45\sin(\tau) \quad (16)$$

$$\text{cc-1-2: } {}^2J_{CH^m}(\text{Hz}) = -3.73 + 1.93\cos(\tau) + 1.60\cos(2\tau) + 0.21\cos(3\tau) - 0.44\sin(\tau) \quad (17)$$

The above relations are in rough agreement with the theoretical results for acetaldehyde,[6] the asymmetry arising from the influence of the hydroxyl group.

There are also substantial changes in $^2J_{CH^m}$ with rotation about the C2−O2 bond, and the co-1-1 and co-1-2 curves are highly asymmetrical. The co-1-1 curve, which describes the changes in the coupling to H2, has minima at −30 and 150° and maxima (of the absolute value) at 60 and −120°; the co-1-2 curve, which describes the coupling to H3, is the mirror image of the co-1-1 curve. For the co-2 rotation path, which differs from co-1 by the rotation of the aldehyde group, the extrema are found at the same dihedral angles but are more shallow. The analytical forms of the dependence of $^2J_{CH^m}$ on the dihedral angle are as follows:

$$\text{co-1-1: } {}^2J_{CH^m}(\text{Hz}) = -3.68 + 0.37\cos(\tau) - 1.06\cos(2\tau) + 0.73\sin(\tau) + 1.52\sin(2\tau) \quad (18)$$

$$\text{co-1-2: } {}^2J_{CH^m}(\text{Hz}) = -3.70 + 0.31\cos(\tau) - 0.96\cos(2\tau) - 0.66\sin(\tau) - 1.47\sin(2\tau) \quad (19)$$

$$\text{co-2-1: } {}^2J_{CH^m}(\text{Hz}) = -2.33 - 1.06\cos(\tau) - 0.18\cos(2\tau) + 0.09\sin(\tau) + 1.19\sin(2\tau) \quad (20)$$

$$\text{co-2-2: } {}^2J_{CH^m}(\text{Hz}) = -2.32 - 0.73\cos(\tau) - 0.42\cos(2\tau) - 0.30\sin(\tau) - 1.30\sin(2\tau) \quad (21)$$

The second $^2J_{CH}$ coupling in glycolaldehyde is $^2J_{CH^a}$ between the aldehyde proton and methylene carbon. To our knowledge, there is no information in the literature on the conformational dependence of this type of geminal coupling. The changes in $^2J_{CH^a}$ during the internal rotation are depicted in Figure 8. There is a strong dependence of $^2J_{CH^a}$ on the dihedral angle determining the conformation about the C1−C2 bond, the changes spanning 16 Hz. The minimum values are assumed by $^2J_{CH^a}$ when the coupled proton is cis to the hydroxyl oxygen (i.e., when $\tau$(H1C1C2O2) = 0°), which is consistent with experimental trends for $^2J_{CH}$ in the H−C−C−X fragment: the cis orientation of the electronegative atom X with respect to the coupled proton makes $^2J_{CH}$ more negative.[6] For the CT structure (cc-1, 180°), the trans orientation of C2−O2 relative to C1−H1 in the aldehyde group increases $^2J_{CH^a}$. By contrast, for the cc-2 path, there is a shallow minimum for the conformation that corresponds to the CC structure despite the same arrangement of the C2−O2 and C1−H1 bonds. There are apparently two competing factors determining the magnitude of $^2J_{CH^a}$: the position of the hydroxyl oxygen and the influence of the hydroxyl proton on the carbonyl group. The latter factor becomes apparent when we consider the dependence of $^2J_{CH^a}$ on $\tau$(H1C1C2O2), which is negligible for the co-1 path but substantial for co-2, with the minimum corresponding to the CC structure (($\tau$(C1C2O2H4)) with the internal hydrogen bond. The changes in $^2J_{CH^a}$ during the internal rotation can be described by the following equations:

$$\text{cc-1: } {}^2J_{CH^a}(\text{Hz}) = 28.92 - 7.91\cos(\tau) + 0.71\cos(2\tau) + 0.73\cos(3\tau) \quad (22)$$

$$\text{co-1: } {}^2J_{CH^a}(\text{Hz}) = 22.80 + 0.08\cos(\tau) - 0.45\cos(2\tau) - 0.08\cos(3\tau) \quad (23)$$

$$\text{co-2: } {}^2J_{CH^a}(\text{Hz}) = 35.14 - 3.07\cos(\tau) - 1.62\cos(2\tau) - 0.12\cos(3\tau) \quad (24)$$

The third $^2J_{CH}$ coupling in glycolaldehyde is $^2J_{CH^h}$ between the hydroxyl proton and methylene carbon. It is difficult to measure, and its changes, depicted in Figure 9, will not be discussed in detail. In relative terms, it exhibits a significant conformational dependence, spanning the range from −1.2 Hz (TT structure) to −3.0 Hz (out-of-plane position of O2−H4 relative to the carbonyl group). The lowest values occur when O2−H4 is coplanar with the heavy atoms (symmetric structures CC, TT, CT, and TS5). On the cc-2 path, a discontinuity in $^2J_{CH^h}$ is visible at $\tau$(H1C1C2O2) = 0°, where cc-2-l and cc-2-r cross. The dependence of $^2J_{CH^h}$ on $\tau$(H1C1C2O2) and $\tau$(C1C2O2H4) can be described as

$$\text{cc-1: } {}^2J_{CH^h}(\text{Hz}) = -1.90 + 0.20\cos(\tau) + 0.43\cos(2\tau) + 0.06\cos(3\tau) \quad (25)$$

$$\text{co-1: } {}^2J_{CH^h}(\text{Hz}) = -1.88 - 0.21\cos(\tau) + 0.39\cos(2\tau) - 0.07\cos(3\tau) \quad (26)$$

$$\text{co-1: } {}^2J_{CH^h}(\text{Hz}) = -2.42 - 0.54\cos(\tau) + 0.27\cos(2\tau) + 0.09\cos(3\tau) \quad (27)$$

*e. $^2J_{HH}$ Geminal Coupling Constant.* It has been known for many years that the geminal $^2J_{HH}$ coupling constants exhibit a strong dependence on the conformation.[6] This is also true for $^2J_{HH}$ in glycolaldehyde, as illustrated in Figure 10.

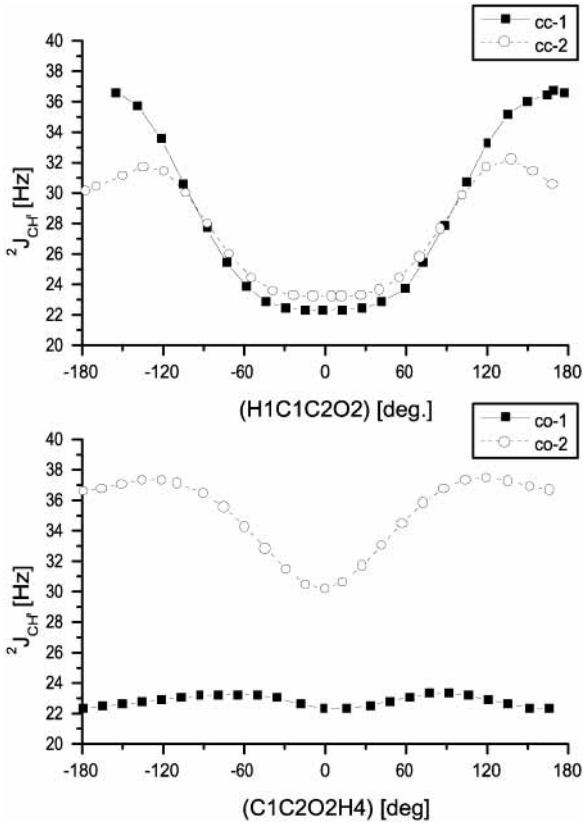


**Figure 8.** $^2J_{CH^a}$ coupling constant (in Hz) as a function of the dihedral angle $\tau$(H1C1C2O2) or $\tau$(C1C2O2H4) (in deg).

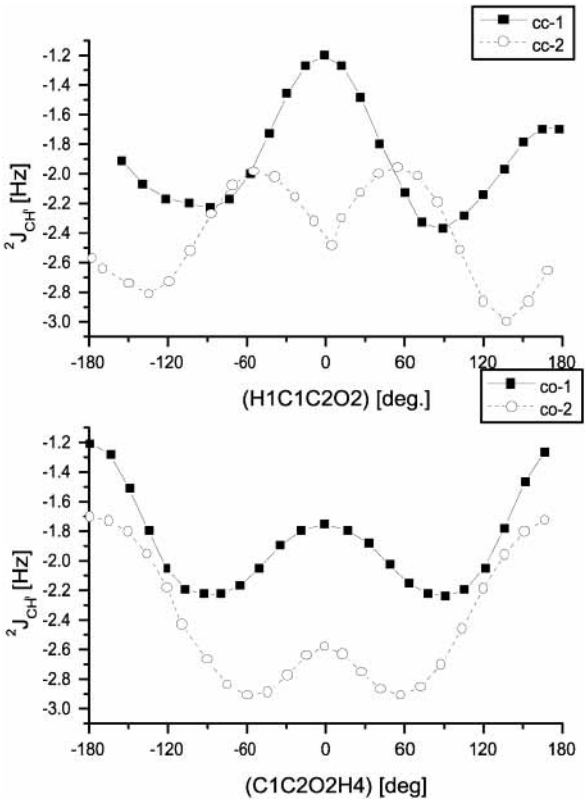


**Figure 9.** $^2J_{CH^b}$ coupling constant (in Hz) as a function of the dihedral angle $\tau$(H1C1C2O2) or $\tau$(C1C2O2H4) (in deg).

The very strong dependence of the $^2J_{HH}$ coupling on $\tau$(H1C1C2O2) (paths cc-1 and cc-2) is typical of the cases where the methylene group is placed α to the carbonyl group.[6] $^2J_{HH}$ is the most negative when the carbonyl group is cis to the C2−O2 bond and trans to the $CH_2$ group ($\tau$(H1C1C2O2) = 180°). Furthermore, when the carbonyl group is trans to the C2−O2 bond ($\tau$(H1C1C2O2) = 0°), the absolute value of $^2J_{HH}$ takes on another (less deep) maximum. The torsional curve is similar for cc-1 and cc-2 and can be described (for cc-1) by the equation

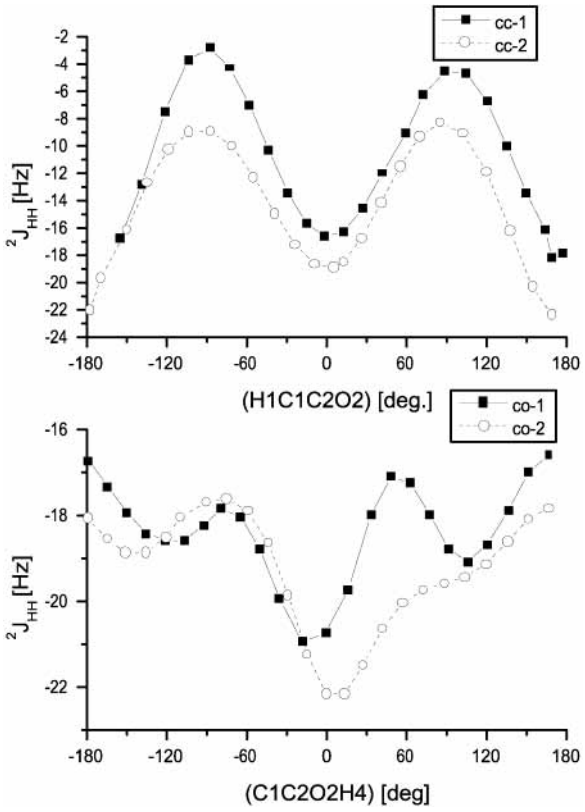


**Figure 10.** $^2J_{HH}$ coupling constant (in Hz) as a function of the dihedral angle $\tau$(H1C1C2O2) or $\tau$(C1C2O2H4) (in deg).

$$\text{cc-1: } {}^2J_{HH}(\text{Hz}) = -10.61 + 0.36\cos(\tau) - 6.85\cos(2\tau) + 0.47\cos(3\tau) \quad (28)$$

The dependence of $^2J_{HH}$ on $\tau$(C1C2O2H4) in paths co-1 and co-2 is smaller than the dependence on $\tau$(H1C1C2O2) but still substantial. For co-1, the largest absolute value of $^2J_{HH}$ occurs when symmetry axis of the methylene group is trans to the O2−H4 bond; the smallest absolute value occurs when the symmetry axis eclipses the O2−H4 bond ($\tau$(C1C2O2H4) = 180°). In addition, local co-1 maxima are observed for $\tau$(C1C2O2H4) ≈ ±120° when O2−H4 eclipses one of the methylene C2−H2-(H3) bonds, and local minima occur for $\tau$(C1C2O2H4) ≈ ±60° when the O−H bond is trans to one of the methylene C−H bonds. For the co-2 curve, the dependence of $^2J_{HH}$ on $\tau$-(C1C2O2H4) is similar to that of the co-1 curve, with some of the extrema becoming points of inflection. The dependence of $^2J_{HH}$ on $\tau$(C1C2O2H4) can be described by the relations

$$\text{co-1: } {}^2J_{HH}(\text{Hz}) = -18.39 - 1.03\cos(\tau) - 0.19\cos(2\tau) - 1.01\cos(3\tau) \quad (29)$$

$$\text{co-2: } {}^2J_{HH}(\text{Hz}) = -2.42 - 0.54\cos(\tau) + 0.27\cos(2\tau) + 0.09\cos(3\tau) \quad (30)$$

The effects of rotation about the C1−C2 and C2−O2 bonds are consistent with what has been found for acetaldehyde[6] and methanol,[6,28] respectively, allowing for complications resulting from the presence of additional fucntional groups in glycolaldehyde.

*f.* $^3J_{HH}$ *Vicinal Coupling Constants.* The angular dependence of the proton−proton vicinal coupling constants in carbohydrate-like systems has been well investigated in the literature (for reviews, see refs 4−6) and is only briefly discussed here. The dependence of the vicinal couplings $^3J_{HH}$ on $\tau$(H1C1C2H2) (or $\tau$(H1C1C2H3)) and $\tau$(H2C2O2H4) (or $\tau$(H2C2O2H4)) is shown in Figure 11. There is practically no influence of the conformation of the aldehyde group on the dependence of $^3J_{HH}$ transmitted through HCOH (co-1 and co-2) or of the O2−H4 position on $^3J_{HH}$ transmitted through HCCH (cc-1 and cc-2): the corresponding curves nearly coincide.

As usual, all curves are bell-shaped. An interesting feature of the torsional dependence of the vicinal $^3J_{HH}$ coupling constants transmitted through either coupling path in glycolaldehyde is the negative sign for dihedral angles between 50 and 100°. (See Figure 11.) This observation is supported by experimental evidence: the proton−proton coupling constant for the gauche conformation in glycolaldehyde has been estimated to be −0.7 Hz.[49] The torsional dependence of $^3J_{HH}$ on $\tau$(H1C1C2H2) or $\tau$(H1C1C2H3) in the case of cc-1 and on $\tau$(H2C2O2H4) or $\tau$(H3C2O2H4) in the case of co-1 and co-2 can be described by the following equations:

$$\text{cc-1-1: } {}^3J_{HH}(\text{Hz}) = 1.69 - 2.26\cos(\tau) + 2.11\cos(2\tau) - 0.38\cos(3\tau) + 0.56\sin(2\tau) \quad (31)$$

$$\text{cc-1-2: } {}^3J_{HH}(\text{Hz}) = 1.72 - 2.22\cos(\tau) + 2.11\cos(2\tau) - 0.40\cos(3\tau) - 0.56\sin(2\tau) \quad (32)$$

$$\text{co-1-1: } {}^3J_{HH}(\text{Hz}) = 5.70 - 2.49\cos(\tau) + 6.36\cos(\tau) + 0.09\cos(3\tau) + 0.03\sin(\tau) \quad (33)$$

$$\text{co-1-2: } {}^3J_{HH}(\text{Hz}) = 5.69 - 2.42\cos(\tau) + 6.34\cos(2\tau) + 0.11\cos(3\tau) - 0.01\sin(\tau) \quad (34)$$

$$\text{co-2-1: } {}^3J_{HH}(\text{Hz}) = 5.48 - 2.39\cos(\tau) + 5.95\cos(2\tau) - 0.01\cos(3\tau) + 0.001\sin(\tau) \quad (35)$$

$$\text{co-2-2: } {}^3J_{HH}(\text{Hz}) = 5.51 - 2.28\cos(\tau) + 5.96\cos(2\tau) - 0.06\cos(3\tau) - 0.11\sin(\tau) \quad (36)$$

*g.* $^3J_{CH}$ *Vicinal Coupling Constant.* Vicinal constant $^3J_{CH}$ (coupling of the carbonyl carbon to the hydroxyl proton) has the expected bell-shaped dependence on the $\tau$(C1C2O2H4) dihedral angle (paths co-1 and co-2), with asymmetry for 0° and 180°. (See Figure 12.) Unlike the case for $^3J_{HH}$, the co-1 and co-2 curves differ significantly. The values of $^3J_{CH}$ vary for 0° and 180° more for the co-1 path than for the co-2 path because $^3J_{CH}$ is also affected by the relative orientation of the carbonyl and hydroxyl groups (rotation about the C1−C2 bond). The $^3J_{CH}$ coupling has a maximum for the TT structure both as a function of $\tau$(C1C2O2H4) (for $\tau$ =180°) and of $\tau$(H1C1C2O2) (cc-1, $\tau$ = 0°). Like the $^3J_{HH}$ couplings, $^3J_{CH}$ is negative for a range of $\tau$(C1C2O2H4) values. The dependence of $^3J_{CH}$ on $\tau$-(H1C1C2O2) and $\tau$(C1C2O2H4) can be expressed as follows:

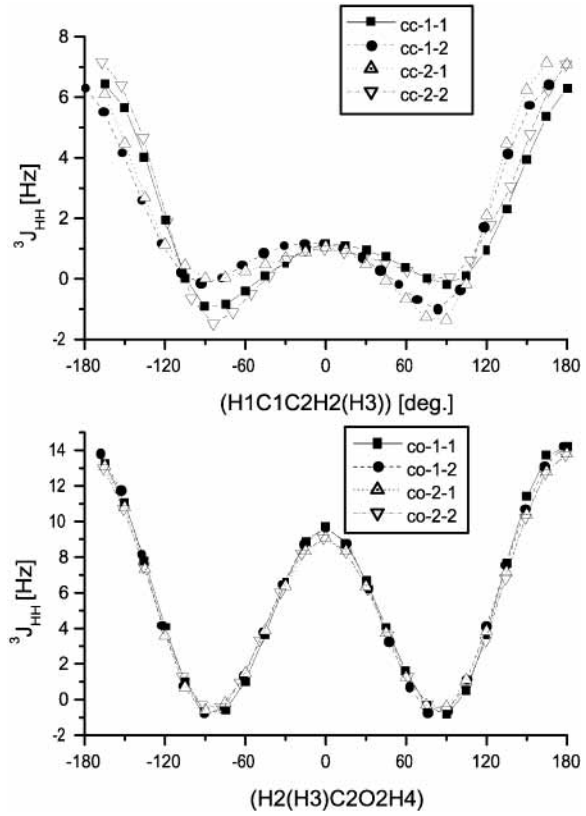


**Figure 11.** $^3J_{HH}$ coupling constant (in Hz) as a function of the dihedral angle $\tau$(H1C1C2H2) (or $\tau$(H1C1C2H3)) or $\tau$(H2C2O2H4) (or $\tau$(H3C2O2H4)) (in deg).

$$\text{cc-1: } {}^3J_{CH}(\text{Hz}) = 10.84 + 1.89\cos(\tau) + 1.27\cos(2\tau) + 0.31\cos(3\tau) \quad (37)$$

$$\text{co-1: } {}^3J_{CH}(\text{Hz}) = 4.39 - 3.45\cos(\tau) + 5.75\cos(2\tau) - 0.67\cos(3\tau) \quad (38)$$

$$\text{co-2: } {}^2J_{CH}(\text{Hz}) = 3.74 - 1.41\cos(\tau) + 4.80\cos(2\tau) - 0.03\cos(3\tau) \quad (39)$$

*h. Long-Range* $^4J_{HH}$ *Coupling Constant.* The last coupling constant discussed here is the four-bond coupling between the aldehyde proton and the hydroxyl proton. Little is known about $^4J_{HH}$ coupling constants transmitted through HCCOH, even though the couplings through HCCCH have long been used for structural assignments.[5]

The changes in $^4J_{HH}$ during rotation about C1−C2 and C2−O2 are illustrated in Figure 13. The coupling changes its sign during the internal rotation, assuming the largest (positive) value for planar structures CC, TS5, and CT. The maximum of 2.25 Hz is observed for the CT structure with a W conformation of the HCCOH fragment, which is consistent with experimental evidence for HCCCH fragments.[5] Despite similar HCCOH conformations, there is a notable difference between the values of $^4J_{HH}$ in the TT (1.0 Hz) and CC (−0.5 Hz) structures. The enhancement of the coupling for the TS5 structure may be caused by through-space interaction because the distance between the coupled protons is only 2.1 Å. The dependence of

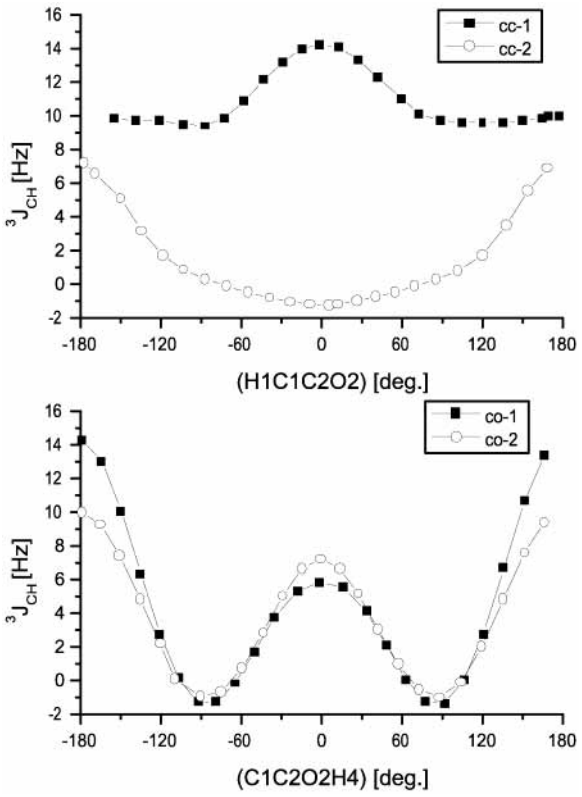


**Figure 12.** $^3J_{CH}$ coupling constant (in Hz) as a function of the dihedral angle $\tau$(H1C1C2O2) or $\tau$(C1C2O2H4) (in deg).

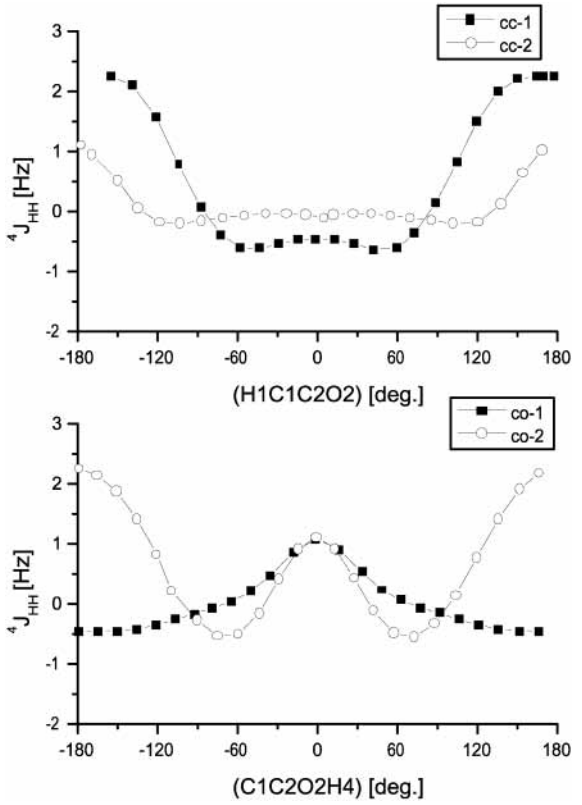


**Figure 13.** $^4J_{HH}$ coupling constant (in Hz) transmitted through the H−C−C−O−H path as a function of the dihedral angle $\tau$(H1C1C2O2) or $\tau$(C1C2O2H4) (in deg).

$^4J_{HH}$ on $\tau$(C1C2O2H4) and $\tau$(H1C1C2O2) can be described by means of the following equations:

$$\text{cc-1: } {}^4J_{HH}(\text{Hz}) = 0.61 - 1.60\cos(\tau) + 0.36\cos(2\tau) + 0.25\cos(3\tau) \quad (40)$$

$$\text{co-1: } {}^4J_{HH}(\text{Hz}) = 0.01 + 0.63\cos(\tau) + 0.22\cos(2\tau) + 0.11\cos(3\tau) \quad (41)$$

$$\text{co-2: } {}^4J_{HH}(\text{Hz}) = 0.64 - 0.84\cos(\tau) + 0.99\cos(2\tau) + 0.24\cos(3\tau) \quad (42)$$

However, because of the strong dependence of $^4J_{HH}$ on both $\tau$(C1C2O2H4) and $\tau$(H1C1C2O2), the usefulness of these relations is limited.

## IV. Summary

We have investigated the conformations and rotational barriers of the glycolaldehyde molecule by means of the MP2 method. The indirect nuclear spin−spin coupling constants have been calculated by means of DFT, and the dependence of the one-bond spin−spin coupling constants $^1J_{CH}$, $^1J_{CC}$, and $^1J_{OH}$, the geminal coupling constants $^2J_{CH}$ and $^2J_{HH}$, and the vicinal coupling constants $^3J_{HH}$ and $^3J_{CH}$ on the $\tau$(CCOH) and $\tau$(HCCO) dihedral angles has been studied. Our results can be summarized as follows:

(1) We have found four minima (CC, TT, TG, and CT) and six saddle points (TS1, TS2, TS3, TS4, TS5, and TS6) on the potential energy surface of glycolaldehyde. The global minimum CC is stabilized by an internal hydrogen bond.

(2) Two transition paths have been investigated for rotation about the C−C bond (cc-1 and cc-2) and for rotation about the C−O bond (co-1 and co-2). Rotation about the C−C bond from the CC to TG structure via TS3 has a barrier of 22.9 kJ/mol. The transformation from TT to CT requires 20.0 kJ/mol, whereas only 12.9 kJ/mol is needed for the opposite transformation. The highest barrier of the rotation about the C−O bond, 23.9 kJ/mol, accompanies the transition from CC to CT via TS2, whereas the transformation from TG to TG* has a much lower barrier of 8.9 kJ/mol. The TG → TT rotation is almost barrierless (2.0 kJ/mol), just like the CT → TT rotation (2.2 kJ/mol). We hope that these results may facilitate the spectral analysis of glycolaldehyde.

(3) We have investigated the dependence of the coupling constants of glycolaldehyde on the dihedral angles, whenever possible comparing the results with theoretical and empirical relationships obtained for similar systems. The calculated coupling constants have been fit by truncated Fourier series with at most five terms. The resulting expressions may help to determine the conformation of carbohydrates and their derivatives from the spin−spin coupling measurements.

(4) In the methodological part of the paper, we have compared the spin−spin coupling constants calculated at the DFT and CCSD levels of theory with each other and with experimental results. In general, the coupling constants calculated by means of DFT are similar to those obtained by CCSD theory; in particular, the DFT method is suitable for studies of the conformational dependence of the spin−spin coupling constants. The largest differences between DFT and CCSD are found for the coupling constants to oxygen ($^1J_{CO}$ and $^1J_{OH}$), in agreement with the general observation that DFT is less reliable for calculations of spin−spin coupling constants of electron-rich atoms.

**Acknowledgment.** We acknowledge support from the 3 TO9A 111 21 KBN grant.

**Supporting Information Available:** Cartesian coordinates of the local minima and transition states optimized at the MP2/aug-cc-pVTZ level and the vibrational frequencies of the local minima. This material is available free of charge via the Internet at http://pubs.acs.org.

## References and Notes


(1) Karplus, M. *J. Chem. Phys.* **1959**, *30*, 11.
(2) Karplus, M. *J. Am. Chem. Soc.* **1963**, *85*, 2870.
(3) Imai, K.; Osawa, E. *Magn. Reson. Chem.* **1990**, *28*, 668.
(4) Minch, M. J. *Concepts Magn. Reson.* **1994**, *6*, 41.
(5) Thomas, W. T. *Prog. NMR. Spectrosc.* **1997**, *30*, 183.
(6) Contreras, R. H.; Peralta, J. E. *Prog. NMR. Spectrosc.* **2000**, *37*, 321.
(7) Haasnoot, C. A. G.; De Leeuw, F. A. A. M.; Altona, C. *Tetrahedron* **1980**, *36*, 2783.
(8) Helgaker, T.; Jaszuński, M.; Ruud, K. *Chem. Rev.* **1999**, *99*, 293.
(9) Fukui, H. *Prog. NMR. Spectrosc.* **1999**, *35*, 267.
(10) Malkin, V. G.; Malkina, O. L.; Salahub, D. R. *Chem. Phys. Lett.* **1994**, *221*, 91.
(11) Dickson, R. M.; Ziegler, T. *J. Phys. Chem.* **1996**, *100*, 5286.
(12) Helgaker, T.; Watson, M.; Handy, N. C. *J. Chem. Phys.* **2000**, *113*, 9402.
(13) Sychrovský, V.; Gräfenstein, J.; Cremer, D. *J. Chem. Phys.* **2000**, *113*, 3530.
(14) Helgaker, T.; Pecul, M. In *Calculation of NMR and EPR Parameters: Theory and Applications*; Kaupp, M., Bühl, M., Malkin, V. G., Eds.; Wiley-VCH: 2004.
(15) Dingley, A. J.; Masse, J. E.; Peterson, R. D.; Barfield, M.; Feigon, J.; Grzesiek, S. *J. Am. Chem. Soc.* **1999**, *121*, 6019.
(16) Barfield, M.; Dingley, A. J.; Feigon, J.; Grzesiek, S. *J. Am. Chem. Soc.* **2001**, *123*, 4014.
(17) Jaszuński, M.; Ruud, K.; Helgaker, T. *Mol. Phys.* **2003**, *101*, 1997.
(18) Hricovini, M.; Malkina, O. L.; Bizik, F.; Nagy, L. T.; Malkin, V. G. *J. Phys. Chem. A* **1997**, *101*, 9756.
(19) Malkina, O. L.; Hricovini, M.; Bizik, F.; Malkin, V. G. *J. Phys. Chem. A* **2001**, *105*, 9188.
(20) Carmichael, I.; Chipman, D. M.; Podlasek, C. A.; Serianni, A. S. *J. Am. Chem. Soc.* **1993**, *115*, 10863.
(21) Perera, S. A.; Bartlett, R. J. *Magn. Reson. Chem.* **2001**, *39*, 183.
(22) Aspiala, A.; Murto, J.; Sténius, P. *Chem. Phys.* **1986**, *106*, 399.
(23) Marstokk, K.-M.; Møllendal, H. *J. Am. Chem. Soc.* **1973**, *16*, 259.
(24) Butler, R. A. H.; De Lucia, F. C.; Petkie, D. T.; Mollendal, M.; Horn, A.; Herbst, E. *Astrophys. J. Suppl.* **2001**, *134*, 319.
(25) Hollis, J. M.; Lovas, F. J.; Jewell, P. R. *Astrophys. J.* **2000**, *540*, 107.
(26) Malkina, O. L.; Salahub, D. R.; Malkin, V. G. *J. Chem. Phys.* **1996**, *105*, 8793.
(27) Pecul, M.; Jaszuński, M.; Sadlej, J. *Chem. Phys. Lett.* **1999**, *305*, 139.
(28) Pecul, M.; Sadlej, J. *Chem. Phys.* **2000**, *255*, 137.
(29) Frisch, M. J.; Trucks, G. W.; Schlegel, H. B.; Scuseria, G. E.; Robb, M. A.; Cheeseman, J. R.; Zakrzewski, V. G.; Montgomery, J. A., Jr.; Stratmann, R. E.; Burant, J. C.; Dapprich, S.; Millam, J. M.; Daniels, A. D.; Kudin, K. N.; Strain, M. C.; Farkas, O.; Tomasi, J.; Barone, V.; Cossi, M.; Cammi, R.; Mennucci, B.; Pomelli, C.; Adamo, C.; Clifford, S.; Ochterski, J.; Petersson, G. A.; Ayala, P. Y.; Cui, Q.; Morokuma, K.; Malick, D. K.; Rabuck, A. D.; Raghavachari, K.; Foresman, J. B.; Cioslowski, J.; Ortiz, J. V.; Stefanov, B. B.; Liu, G.; Liashenko, A.; Piskorz, P.; Komaromi, I.; Gomperts, R.; Martin, R. L.; Fox, D. J.; Keith, T.; Al-Laham, M. A.; Peng, C. Y.; Nanayakkara, A.; Gonzalez, C.; Challacombe, M.; Gill, P. M. W.; Johnson, B. G.; Chen, W.; Wong, M. W.; Andres, J. L.; Head-Gordon, M.; Replogle, E. S.; Pople, J. A. *Gaussian 98*, revision A.1; Gaussian, Inc.: Pittsburgh, PA, 1998.
(30) Dunning, T. H. *J. Chem. Phys.* **1989**, *90*, 1007.
(31) Kendall, R. A.; Dunning, T. H.; Harrison, R. J. *J. Chem. Phys.* **1992**, *96*, 6796.
(32) Becke, A. D. *J. Chem. Phys.* **1993**, *98*, 5648.
(33) Stephens, P. J.; Devlin, F. J.; Chabalowski, C. F.; Frisch, M. J. *J. Phys. Chem.* **1994**, *98*, 11623.
(34) Helgaker, T.; Jensen, H. J. A.; Jørgensen, P.; Olsen, J.; Ruud, K.; Ågren, H.; Auer, A. A.; Bak, K. L.; Bakken, V.; Christiansen, O.; Coriani, S.; Dahle, P.; Dalskov, E. K.; Enevoldsen, T.; Fernandez, B.; Hättig, C.; Hald, K.; Halkier, A.; Heiberg, H.; Hettema, H.; Jonsson, D.; Kirpekar, S.; Kobayashi, R.; Koch, H.; Mikkelsen, K. V.; Norman, P.; Packer, M. J.; Pedersen, T. B.; Ruden, T. A.; Sanchez, A.; Saue, T.; Sauer, S. P. A.; Schimmelpfenning, B.; Sylvester-Hvid, K. O.; Taylor, P. R.; Vahtras, O. *DALTON: An ab Initio Electronic Structure Program*, release 1.2, 2001. See http://www.kjemi.uio.no/software/dalton/dalton.html.
(35) Auer, A. A.; Gauss, J. *J. Chem. Phys.* **2001**, *115*, 1619.
(36) Stanton, J. F.; Gauss, J.; Watts, J. D.; Lauderdale, W. J.; Bartlett, R. J. *Int. J. Quantum Chem.: Quantum Chem. Symp.* **1992**, *26*, 879.
(37) Szalay, P. G.; Gauss, J.; Stanton, J. *Theor. Chem. Acc.* **1998**, *100*, 5.
(38) Schindler, M.; Kutzelnigg, W. *J. Chem. Phys.* **1982**, *76*, 1919.
(39) Helgaker, T.; Jaszuński, M.; Ruud, K.; Górska, A. *Theor. Chem. Acc.* **1998**, *99*, 175.
(40) Pecul, M.; Helgaker, T. *Int. J. Mol. Sci.* **2003**, *4*, 143.
(41) Pecul, M.; Sadlej, J.; Helgaker, T. *Chem. Phys. Lett.* **2003**, *372*, 476.
(42) Barone, V.; Peralta, J. E.; Contreras, R. H.; Snyder, J. P. *J. Phys. Chem. A* **2002**, *106*, 5607.
(43) Berger, S.; Braun, S.; H.-O. Kalinowski. *NMR-Spectroskopie von Nichtmetallen. band 1: Grundlagen, $^{17}O$-, $^{33}S$ und $^{129}Xe$-Spectroskopie*; Georg Thieme Verlag Stuttgart: New York, 1992.
(44) Perlin, A. S.; Casu, B. *Tetrahedron Lett.* **1969**, 2921.
(45) Peralta, J. E.; Scuseria, G. E.; Cheeseman, J. R.; Frisch, M. J. *Chem. Phys. Lett.* **2003**, *375*, 452.
(46) Vizioli, C.; de Azúa, M. C. R.; Giribet, C. G.; Contreras, R. H.; Turi, L.; Danenberg, J. J.; Rae, I. D.; Weigold, J. A.; Malagoli, M.; Zanasi, R.; Lazzeretti, P. *J. Phys. Chem.* **1994**, *98*, 8858.
(47) Giribet, C. G.; Vizioli, C.; de Azúa, M. C. R.; Contreras, R. H.; Danenberg, J. J.; Masunov, A. *J. Chem. Soc., Faraday Trans.* **1996**, *92*, 3029.
(48) Barfield, M.; Johnston, M. D., Jr. *Chem. Rev.* **1973**, *73*, 53.
(49) Laatikainen, R.; Král, V.; Äyräs, P. *J. Magn. Reson.* **1987**, *74*, 12.